

Formation and local structure of framework Al Lewis sites in beta zeolites

Cite as: J. Chem. Phys. **156**, 104702 (2022); <https://doi.org/10.1063/5.0083666>

Submitted: 28 December 2021 • Accepted: 15 February 2022 • Accepted Manuscript Online: 15 February 2022 • Published Online: 08 March 2022

 Libor Kobera,  Jiri Dedecek, Petr Klein, et al.



View Online



Export Citation



CrossMark

ARTICLES YOU MAY BE INTERESTED IN

[Explaining the structure sensitivity of Pt and Rh for aqueous-phase hydrogenation of phenol](#)

The Journal of Chemical Physics **156**, 104703 (2022); <https://doi.org/10.1063/5.0085298>

[Identification of metal-sensitive structural changes in the Ca²⁺-binding photocomplex from *Thermochromatium tepidum* by isotope-edited vibrational spectroscopy](#)

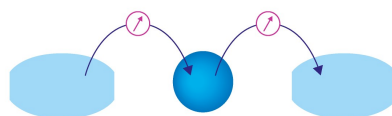
The Journal of Chemical Physics **156**, 105101 (2022); <https://doi.org/10.1063/5.0075600>

[The effect of explicit counterion binding on the transference number of polyelectrolyte solutions](#)

The Journal of Chemical Physics **156**, 104901 (2022); <https://doi.org/10.1063/5.0083414>

Webinar

Interfaces: how they make
or break a nanodevice



March 29th – Register now

 Zurich
Instruments

Formation and local structure of framework Al Lewis sites in beta zeolites

Cite as: J. Chem. Phys. 156, 104702 (2022); doi: 10.1063/5.0083666

Submitted: 28 December 2021 • Accepted: 15 February 2022 •

Published Online: 8 March 2022



View Online



Export Citation



CrossMark

Libor Kobera,¹  Jiri Dedecek,²  Petr Klein,²  Edyta Tabor,²  Jiri Brus,¹  Anna V. Fishchuk,²
and Stepan Sklenak^{2,a)} 

AFFILIATIONS

¹ Institute of Macromolecular Chemistry of the Czech Academy of Sciences, Heyrovský nám. 2, CZ 162 06 Prague 6, Czech Republic

² J. Heyrovský Institute of Physical Chemistry of the Czech Academy of Sciences, Dolejškova 3, CZ 182 23 Prague 8, Czech Republic

^{a)} Author to whom correspondence should be addressed: stepan.sklenak@jh-inst.cas.cz

ABSTRACT

Framework Al_{FR} Lewis sites represent a substantial portion of active sites in H-BEA zeolite catalysts activated at low temperatures. We studied their nature by ²⁷Al WURST-QCPMG nuclear magnetic resonance (NMR) and proposed a plausible mechanism of their formation based on periodic density functional theory calculations constrained by ¹H MAS, ²⁷Al WURST-QCPMG, and ²⁹Si MAS NMR experiments and FTIR measurements. Our results show that the electron-pair acceptor of Al_{FR} Lewis sites corresponds to an Al_{TRI} atom tricoordinated to the zeolite framework, which adsorbs a water molecule. This Al_{TRI}-OH₂ complex is reflected in ²⁷Al NMR resonance with $\delta_{\text{iso}} = 70 \pm 5$ ppm and $C_Q = 13 \pm 2$ MHz. In addition, the Al_{TRI} atom with adsorbed acetonitrile-*d*₃ (the probe of Al_{FR} Lewis sites in FTIR spectroscopy) exhibits a similar ²⁷Al NMR resonance. We suggest that these Al_{FR} Lewis sites are formed from Al-OH-Si-O-Si-O-Si-OH-Al sequences located in 12-rings (i.e., close unpaired Al atoms).

Published under an exclusive license by AIP Publishing. <https://doi.org/10.1063/5.0083666>

I. INTRODUCTION

Zeolites are crystalline microporous aluminosilicate molecular sieves. They are made of corner-sharing TO₄ tetrahedra (T = Si, Al⁺). Silicon-rich zeolites (most of them belonging to the pentasil-ring zeolites) with Si/Al > 8 represent the most important group of heterogeneous industrial catalysts. Besides Brønsted acid SiO-HAl groups formed by protons compensating tetrahedral AlO₄⁻, electron-pair acceptor Al Lewis sites are often present in zeolite catalysts.¹⁻³ The Al Lewis sites were suggested to correspond to Al centers tricoordinated to the zeolite framework.³⁻⁷ However, this type of Al has resisted detection by ²⁷Al MAS nuclear magnetic resonance (NMR) until 2015.⁸ While the formation of Al Lewis sites related to extra-framework (Al_{EF}) atoms can be controlled by the zeolite treatment, the detailed structure, origin, and possibility of the regulation of the creation of Al_{FR} Lewis sites related to framework Al atoms (Al_{FR}) are not clear despite their importance. Typically, the presence of Al_{FR} Lewis sites significantly affects the selectivity of transformations of hydrocarbons and causes

a formation of undesired polyaromatic deposits. Conversely, Al_{FR} Lewis sites can represent the active sites as for example, in the Meerwein-Ponndorf-Verley reduction of ketones to alcohols over zeolites.⁹

A significant effort has been spent to elucidate the presence, structure, and origin of Al_{FR} Lewis sites in zeolites active in catalytic processes. However, IR spectroscopy provided only indirect evidence of the formation of Al_{FR} Lewis sites in various zeolite structures.^{5,10,11} Only a K-edge x-ray absorption spectroscopy (XAS) study indicated the presence of a low amount (10% of Al at 700 °C) of tricoordinated Al_{FR}, attributable to Al_{FR} Lewis sites in dehydrated beta zeolites.⁷

Beta zeolites possess a unique topology with an interconnected 3D pore system having the largest pore diameter among aluminosilicates. Matrices with the *BEA structure belong to the silicon-rich zeolites with the highest impact in industrial catalysis (USY > ZSM-5 > mordenite > the beta zeolite). Aluminosilicates with the *BEA framework are the most prone among the pentasil-ring zeolites to massively form Al_{FR} Lewis sites (up to 40%–60% of the acid sites)

even at 450 °C due to the special topology of their framework and the unique Al distribution.^{9,12}

We have recently shown that Al_{FR} Lewis sites formed as minor species created under 300 °C in a zeolite of the ferrierite (FER) structure are formed by dehydroxylation of terminal $-(\text{SiO})_3\text{-AlOH}$ entities tricoordinated to the zeolite framework. The Al_{FR} Lewis sites are reflected in an extremely broad ²⁷Al NMR resonance with $\delta_{\text{iso}} \approx 67$ ppm and $C_Q \approx 20$ MHz. Such terminal Al_{FR} Lewis sites are located at internal or external surfaces and are accessible to probe molecules and reactants. However, there is a substantial discrepancy between the observed C_Q value of 20 MHz and that of 35 MHz predicted for the near planar Al tricoordinated to the zeolite framework.⁸ This issue required a further investigation. Details regarding this issue are provided in Sec. III. F. Conversely, $-(\text{SiO})_3\text{-AlOH}$ entities were not reported for beta zeolites, and moreover, Al_{FR} Lewis sites prevailing in beta zeolites are formed at higher temperatures compared to those created in the ferrierite zeolite. Therefore, the structure of Al_{FR} Lewis sites in the beta zeolite remains unknown.

In this article, we describe the investigation of the formation and local structure of the Al_{FR} Lewis sites in the beta zeolite employing ²⁷Al WURST-QCPMG, ²⁹Si MAS, and ¹H MAS NMR experiments and FTIR measurements in tandem with extensive periodic density functional theory (DFT) calculations including molecular dynamics (MD). We show that the electron-pair acceptor of Al_{FR} Lewis sites corresponds to an Al_{TRI} atom tricoordinated to the zeolite framework, which adsorbs a water molecule. Furthermore, a plausible mechanism of the formation of these Al_{FR} Lewis sites from Al-OH-Si-O-Si-O-Si-OH-Al sequences of the zeolite framework is suggested.

II. EXPERIMENTAL SECTION

A. Sample preparation and treatment

The beta zeolite (Si/Al 11.3, containing a template) was kindly supplied by Zeolyst International (CP 814B-25, Lot. No. 814B-25-1597-77). It was heated in an ammonia stream at 420 °C for 3 h to remove the template according to the procedure of van der Waal *et al.*,¹³ preserving Al atoms in the framework. The NH₄-BEA sample was subsequently deammoniated in a stream of O₂ at 520 °C for 2 h to give the H-BEA form. The distribution of Al atoms in the framework is described in our prior study.¹²

B. FTIR spectroscopy

FTIR spectra were measured using an FTIR spectrometer (Nicolet 6700) equipped with LN₂ cooled detector. FTIR spectra were recorded at ambient laboratory temperature between 4000 and 400 cm⁻¹ with a single spectrum consisting of 128 scans at a resolution of 2 cm⁻¹. The samples were evacuated (10⁻³ Pa) at 500 °C for 3 h before the measurements.

C. Quantitative analysis of the Brønsted and Al_{FR} Lewis acid sites

10 Torr of acetonitrile-*d*₃ was adsorbed on the sample at ambient laboratory temperature for 30 min followed by a 30-min desorption at ambient laboratory temperature to quantitatively

analyze the Brønsted and Al_{FR} Lewis acid sites. The FTIR spectrum after the acetonitrile-*d*₃ adsorption (Fig. S1 of the [supplementary material](#)) was analyzed, employing the previously established method¹⁴ based on the deconvolution of the spectrum in the region 2360–2200 cm⁻¹ into four components. The low intense bands at 2250 and 2280 cm⁻¹ are assigned to physisorbed acetonitrile-*d*₃ on the beta zeolite sample surface and silanol groups SiOH, respectively. The maxima at 2297 and 2324 cm⁻¹ characterize the Brønsted and Al_{FR} Lewis, respectively, acid sites. The concentrations of these acid sites were calculated using following extinction coefficients: 2.05 cm μmol⁻¹ for Brønsted acid sites and 3.62 cm μmol⁻¹ for Al_{FR} Lewis acid sites, and they are listed as follows:

$$[\text{Brønsted}] = 0.54 \text{ mmol/g,}$$

$$[\text{Al}_{\text{FR}} \text{ Lewis}] = 0.33 \text{ mmol/g.}$$

Because the concentration of Al in the zeolite is $[\text{Al}] = 1.35$ mmol/g, at least two Brønsted sites are required for the formation of one Al_{FR} Lewis site as $[\text{Al}] = [\text{Brønsted}] + 2.4[\text{Al}_{\text{FR}} \text{ Lewis}]$.

D. Characterization of the OH groups

The FTIR spectrum of evacuated samples (10⁻³ Pa) at 500 °C for 3 h was collected (Fig. S2 of the [supplementary material](#)) to qualitatively analyze the terminal SiOH groups and Brønsted acid sites SiOHAl. The well resolved bands at 3743 and 3611 cm⁻¹ are typical for terminal silanol groups SiOH and Brønsted acid sites SiOHAl, respectively. The broad band centered around 3500 cm⁻¹ reflects the presence of so called perturbed SiOHAl acid sites. Note that the extinction coefficients are not known, and therefore, this region of FTIR spectra of the dehydrated zeolite cannot be employed for quantitative or semi-quantitative analysis of the SiOH and SiOHAl groups.

E. MAS NMR spectroscopy

Solid state NMR experiments were carried out on a Bruker Avance 500 MHz (11.7 T) Wide Bore spectrometer using either 4 or 3.2 mm double-resonance probes. Samples were packed into 4 and 3.2 mm o.d. ZrO₂ rotors and sealed with Kel-F caps. The dehydrated samples were prepared by *in situ* evacuation (10⁻³ Pa) in the NMR rotors at 500 °C for 4 h and sealing in the rotor under *in situ* conditions. The sample with adsorbed acetonitrile-*d*₃ was prepared by the adsorption of 10 Torr of acetonitrile-*d*₃ on the evacuated sample (see the above-mentioned) at ambient laboratory temperature for 30 min followed by a 30-min desorption at ambient laboratory temperature. Then, the sample was sealed out under *in situ* conditions.

The single pulse ¹H MAS NMR spectrum of the dehydrated sample was recorded using the 3.2 mm probe at a rotation frequency of 20 kHz using the spin-echo approach [$\pi/2-(t_1)-\pi\text{-aq.}$], where the t_1 delay was rotor synchronized (1 loop). The recycle delay was 2 s. The ¹H chemical shifts were referenced to adamantane (1.85 ppm).

The ²⁷Al MAS NMR spectra of the hydrated samples were acquired using the 4 mm probe at a rotation frequency of 12 kHz, employing a high-power decoupling pulse sequence (SPINAL64) with a $\pi/12$ excitation pulse length of 0.4 μs and a recycle delay of

2 s. The ^{27}Al isotropic chemical shifts were referenced to the aqueous solution of $\text{Al}(\text{NO}_3)_3$ (0.0 ppm).

^{29}Si MAS NMR spectra of the hydrated and dehydrated samples were measured in the 4 mm probe using a $\pi/2$ excitation pulse length of 4 μs with a recycle delay of 30 s at a rotation frequency of 7 kHz. The ^{29}Si chemical shifts were referenced to M_8Q_8 (-108.9 ppm, the highest field signal). Analytical simulations of NMR spectra were performed using the Dmfit program.¹⁵

F. ^{27}Al WURST-QCPMG NMR experiments

The measurements of the dehydrated samples were carried out using ^{27}Al WURST-QCPMG NMR spectroscopy. Both ^{27}Al WURST-QCPMG and BRAIN-CP/WURST-QCPMG NMR spectra were collected under static conditions on a 11.7 T Bruker AVANCE III HD spectrometer. A 4 mm cross-polarization magic angle spinning (CP/MAS) probe was used for ^{27}Al experiments at the Larmor frequency of $\nu(^{27}\text{Al}) = 130.328$ MHz. WURST-QCPMG¹⁶ and BRAIN-CP/WURST-QCPMG¹⁷ experiments were carried out using a CT-selective 50 μs WURST pulse with 48 loops, and the recycle delay was 4 s.

G. Quantification of the concentrations of the silanol groups

The ^1H MAS NMR spectrum (Fig. 1) allows for only determination of the ratio between the OH groups of (i) the SiOH and $\text{Si}(\text{OH})_2$ silanol groups and (ii) the Brønsted acid sites SiOHAl.

Our DFT computations reveal that one proton of the water molecule adsorbed on the Al_{TRI} atom is similar to that of the Brønsted acid sites SiOHAl while the other hydrogen atom to H of SiOH and $\text{Si}(\text{OH})_2$ silanol groups. Therefore, the ^1H NMR signal of (i) the former proton can be added to the ^1H NMR signal at around 3.8 ppm (including the shoulder at around 5 ppm) and (ii) the latter one to the ^1H NMR signal of SiOH and $\text{Si}(\text{OH})_2$ silanol groups at around 1.6 ppm. Note that the extinction coefficients of the ^1H NMR resonances of the single pulse ^1H MAS NMR spectrum of

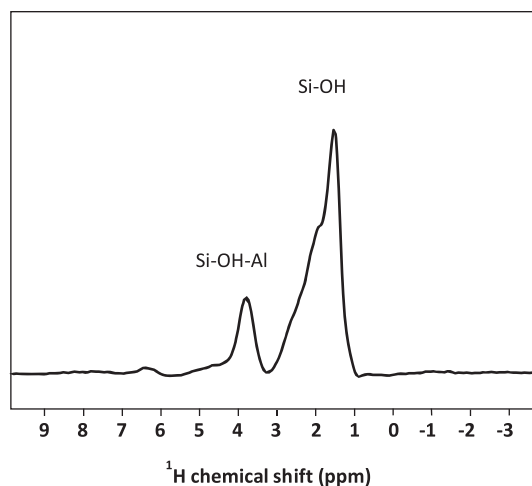


FIG. 1. ^1H MAS NMR spectrum of the dehydrated H-BEA zeolite recorded using a "spin-echo" sequence (1 loop) at 20 kHz.

TABLE I. The concentration of the Al atoms, the Brønsted (B) and Al_{FR} Lewis (L) acid sites, the $\text{Si}(3\text{Si},1\text{OH})$ and $\text{Si}(2\text{Si},2\text{OH})$ atoms (Si_{OH}), and the silanol SiOH groups (OH_{Si}) in the hydrated and dehydrated beta zeolite samples and the values predicted for one (mechanism I) and two (mechanism II) Si atoms partly released from the framework.

	Al ^{a,b}	B ^{a,c}	L ^{a,d}	Si_{OH} ^{a,e}	OH_{Si} ^{a,f}
NH_4 -BEA/hydr	1.35	g	h	0.95	0.95
H-BEA/deh	1.35	0.54	0.33	1.87	2.16
Mechanism I ⁱ				1.94	2.60
Mechanism II ⁱ				2.93	3.92

^aIn mmol/g.

^bFrom chemical analysis.

^cFrom FTIR of adsorbed acetonitrile- d_3 on the Brønsted acid SiOHAl groups.

^dFrom FTIR of adsorbed acetonitrile- d_3 on the Al_{FR} Lewis sites.

^e Si_{OH} from ^{29}Si MAS NMR.

^f OH_{Si} in the NH_4 -BEA/hydr sample equal to Si_{OH} (only terminal SiOH) and OH_{Si} in the H-BEA/deh sample from ^1H MAS NMR calibrated using FTIR of adsorbed acetonitrile- d_3 on the Brønsted SiOHAl groups.

^gNot determined in the hydrated zeolite.

^hNot formed in the hydrated zeolite.

ⁱValues calculated for B = 0.54 and L = 0.33 mmol/g.

the OH groups are identical. The calibration of the Brønsted acid groups SiOHAl is required for quantitative analysis of the SiOH and $\text{Si}(\text{OH})_2$ silanol groups using ^1H MAS NMR. The concentration of the Brønsted acid sites SiOHAl of 0.54 mmol/g (Table I) obtained from FTIR spectroscopy of acetonitrile- d_3 adsorbed on the Brønsted acid sites SiOHAl was employed.

III. COMPUTATIONAL DETAILS

A. Electronic structure calculations

Periodic DFT calculations were carried out employing the Vienna Ab initio Simulation Package (VASP) code.^{18–21} The Kohn–Sham equations were solved variationally in a plane-wave basis set using the projector-augmented wave (PAW) method of Blöchl²² as adapted by Kresse and Joubert.²³ The exchange–correlation energy was described by the PW91 generalized gradient approximation (GGA) functional,^{24,25} which has been successfully employed in our previous studies.^{26–31} Brillouin zone sampling was restricted to the Γ -point. A plane-wave cutoff of 400 eV was employed for geometry optimizations, while a smaller cutoff of 300 eV was used for the molecular dynamics simulations.

B. Geometry optimizations

The atomic positions were optimized by employing a conjugate-gradient algorithm minimization of energies and forces while the lattice parameters were fixed (constant volume) at their experimental values.

C. Molecular dynamics

The molecular dynamics (MD) simulations used the exact Hellmann–Feynman forces acting on atoms and applied the statistics of the canonical ensemble to the motion of the atomic nuclei³² using the Verlet velocity algorithm^{33,34} to integrate Newton's equations of motion. The time step for the integration of the equations of

motion was 1 fs. The simulations were run for 10 000 fs at 400 K for the models as follows: (i) the Al_{FR} Lewis site with a 3-ring (one partly released Si' atom, Scheme I), (ii) the same model with CD_3CN adsorbed on the Al' atom, (iii) the same model with H_2O adsorbed on the Al' atom, (iv) the same model with N_2 adsorbed on the Al' atom, (v) the Al_{FR} Lewis site with a 3-ring (two partly released Si' and Si'' atoms, Scheme II), (vi) the same model with CD_3CN adsorbed on the Al' atom, (vii) the Al_{FR} Lewis site with a 4-ring (two partly released Si' and Si'' atoms, Scheme SIII of the supplementary material), and (viii) the same model with CD_3CN adsorbed on the Al' atom. Visual inspection of the structures along the MD trajectories showed that the duration of the MD simulations was long enough because it included both the rearrangements of the structures as well as a long period when the system fluctuated around the equilibrium and “snapshots” were collected and optimized. Similar time lengths were used for MD simulations in our prior studies of zeolites.^{12,27,28,30,31,35,36} The MD simulations serve to obtain the rearranged local structures. The rearrangement can be monitored by visual inspection. No physical quantity is derived from the MD trajectories. The structures of 20 distinct “snapshots” collected at 500, 1000, 1500, . . . , 10 000 fs of the molecular dynamics simulations were optimized for the eight models. The most stable structures for the models (i–iv) were used for the

subsequent calculations of the ^{27}Al NMR parameters. The starting geometry (P1 symmetry) of the models was generated from the experimental orthorhombic structure of polymorph A of the beta zeolite (<http://www.iza-structure.org/databases>, supercell composed of two-unit cells, cell parameters, $a = 12.632$, $b = 25.264$, and $c = 26.186$ Å).

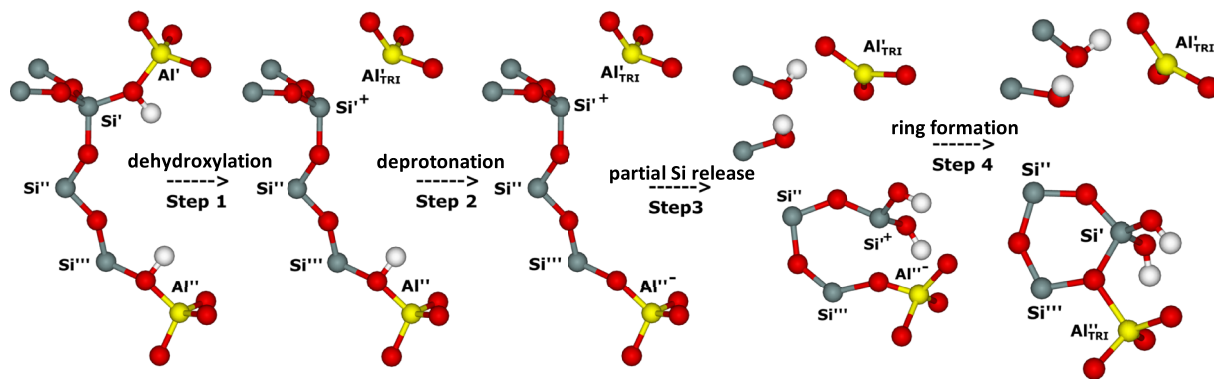
Using MD simulations or other similar global optimization techniques, which allow for the structural rearrangement, is necessary^{27,28} as there are no available experimental structures of the beta zeolites with Al_{FR} Lewis sites.

D. Calculations of the SiOHAl Brønsted acid sites

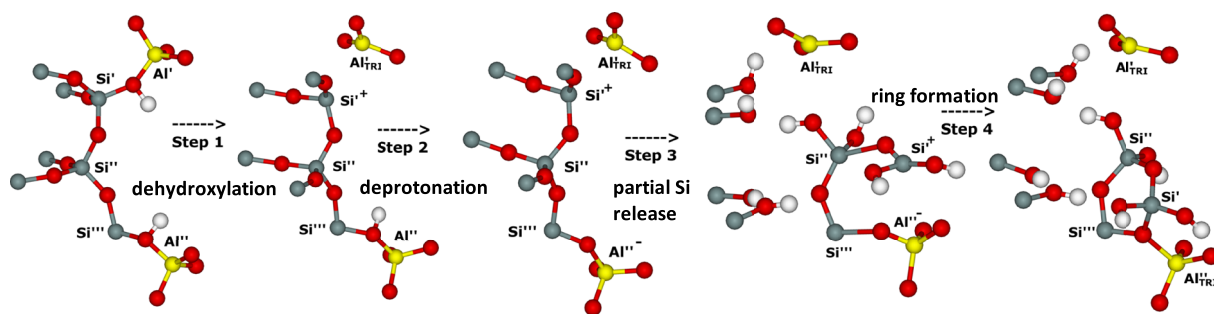
The eight models of the SiOHAl Brønsted acid sites corresponding to the protonation of one of the four symmetrically inequivalent oxygen atoms of the $\text{Al}'\text{O}_4^-$ and $\text{Al}''\text{O}_4^-$ tetrahedra were calculated. The same starting geometry was employed, and the structures of the eight models of SiOHAl were optimized.

E. Calculations of ^{27}Al NMR parameters

Clusters of seven coordination shells around the Al atom of interest ($\text{Al}-\text{O}-\text{Si}-\text{O}-\text{Si}-\text{O}-\text{Si}-\text{O}-\text{H}_{\text{link}}$) were extracted from the



SCHEME I. Mechanism I: the formation the Al_{FR} Lewis site with one Si atom partly released from the zeolite framework from an $\text{Al}'\text{-OH-Si}'\text{-O-Si}''\text{-O-Si}'''\text{-OH-Al}''$ sequence. Only the atoms of interest are displayed. Silicon atoms are in gray, oxygen atoms in red, aluminum atoms in yellow, and hydrogen atoms in white.



SCHEME II. Mechanism II: the formation of the Al_{FR} Lewis site with two Si atoms partly released from the zeolite framework from an $\text{Al}'\text{-OH-Si}'\text{-O-Si}''\text{-O-Si}'''\text{-OH-Al}''$ sequence. Only the atoms of interest are displayed. Silicon atoms are in gray, oxygen atoms in red, aluminum atoms in yellow, and hydrogen atoms in white.

fully relaxed structures to calculate, employing the Gaussian09 program,³⁷ ²⁷Al NMR shielding tensors; nuclear quadrupolar coupling constants³⁸ C_Q ; and asymmetry parameters³⁸ η for the ²⁷Al atom by the gauge independent atomic orbital method (GIAO)³⁹ using the B3LYP functional^{40,41} and the pcS basis sets of Jensen.⁴² pcS-4 for the Al atom and pcS-1 for all the other atoms. The EFGShield program³⁸ was employed to extract the C_Q and η values from the Gaussian output files. The calculated Al shieldings were converted to Al isotropic chemical shifts, employing the experimental and theoretical NMR parameters obtained for the silicon-rich structure of chabazite (²⁷Al NMR shielding of 510 ppm = ²⁷Al isotropic chemical shift of 60 ppm).^{43,44}

F. Al_{FR} Lewis sites in the ferrierite zeolite

We have recently shown that Al_{FR} Lewis sites formed as minor species created under 300 °C in a zeolite of the FER structure are formed by dehydroxylation of terminal $-(\text{SiO})_3\text{-AlOH}$ entities tricoordinated to the zeolite framework.⁸ The Al_{FR} Lewis sites are reflected in an extremely broad ²⁷Al NMR resonance with $\delta_{iso} \approx 67$ ppm and $C_Q \approx 20$ MHz.⁸ Such terminal Al_{FR} Lewis sites are located at internal or external surfaces and are accessible to probe molecules and reactants. However, there is a substantial discrepancy between the observed C_Q value of 20 MHz and that of 35 MHz predicted for the near planar Al tricoordinated to the zeolite framework.⁸ Based on this study of the beta zeolite, we conclude that the observed extremely broad ²⁷Al NMR resonance ($\delta_{iso} \approx 67$ ppm and $C_Q \approx 20$ MHz) for the ferrierite zeolite⁸ corresponds to Al_{FR} Lewis sites tricoordinated to the zeolite framework with adsorbed H₂O. Our calculations yielded $\delta_{iso} = 59$ ppm and $C_Q = 16.7$ MHz for this site using the same computational approach as in our prior study.⁸ These theoretical values are in good agreement with the experiment.

IV. RESULTS

FTIR spectroscopy of acetonitrile-*d*₃ adsorbed on the H-BEA sample (Fig. S1 of the [supplementary material](#)) (i) showed a significant formation of Al_{FR} Lewis sites (reaching 28% of the acid sites, see [Table I](#)) in the zeolite sample dehydrated at 500 °C, which is a typical temperature for the creation of Al_{FR} Lewis sites in beta zeolites, and (ii) confirmed a well-known fact that one Al_{FR} Lewis site is formed at the expense of two Brønsted acid SiOHAl sites.¹²

Two possible mechanisms of the formation of Al_{FR} Lewis sites were extensively considered in the past: (i) cleavage of the Al–O bond and the subsequent formation of tricoordinated Al_{FR} and SiOH and (ii) dehydroxylation of one Brønsted acid SiOHAl group and deprotonization of another close SiOHAl (Fig. S3 of the [supplementary material](#)). Regarding (i), our DFT calculations including molecular dynamics show that when the Al–O bond is broken, it is immediately rebuilt. The zeolite framework cannot rearrange to maintain the Al atom tricoordinated to the zeolite framework. Concerning (ii), the structure features one tricoordinated Al_{FR} and also one tricoordinated Si⁺ atom, which is remotely balanced by the deprotonated Brønsted site. This structure cannot correspond to the Al_{FR} Lewis site either since the Al atom tricoordinated to the zeolite framework is not accessible to probe molecules and reactants. In addition, tricoordinated Si⁺ atoms are extremely unstable and must

be immediately transformed into some more stable structure blocking the access to the Al_{TR1} atom even more. Therefore, the dehydroxylation of the SiOHAl group most likely represents only the first step in the formation of Al_{FR} Lewis site, and a partial release of Si atoms from the zeolite framework is proposed as a key step for the formation of stable and accessible Al_{FR} Lewis sites.

The ²⁹Si MAS NMR measurements of (i) the hydrated parent sample (NH₄-BEA), (ii) the calcined and rehydrated sample (H-BEA), and (iii) the calcined, rehydrated, and subsequently equilibrated with NaNO₃ sample (NaH-BEA) show very similar Si/Al_{FR} ratios: 11.8, 12.0, and 11.8, respectively (Fig. S5 of the [supplementary material](#)), which, moreover, agree well with the Si/Al ratio obtained from chemical analysis (Si/Al 11.3). These results clearly show that the calcination is connected with no release of Al from the zeolite framework. Our ²⁷Al MAS NMR experiments on (i) the hydrated parent sample (NH₄-BEA) and (ii) the calcined, rehydrated, and subsequently equilibrated with NaNO₃ sample (NaH-BEA) reveal that the two materials do not exhibit the presence of extra-framework Al (Fig. S6 of the [supplementary material](#)). This guarantees that the Al_{FR} Lewis sites represent the only type of Al Lewis centers in the investigated dehydrated sample. In addition, the ²⁹Si CP MAS NMR spectrum of the dehydrated H-BEA sample (Fig. S7 of the [supplementary material](#)) clearly reveals the absence of Si(1Si,3OH) and Si(0Si,4OH) atoms. This excludes a release of various Si species [i.e., “free” Si(OH)₄, (OH)₃Si–O–Si(OH)₃, and (OH)₃Si–O–[Si(OH)₂]_{n≥1}–O–Si(OH)₃] from the zeolite framework.

The *BEA structure is very unique among the pentasil-ring zeolites regarding the massive formation of Al_{FR} Lewis sites at lower temperatures.^{9,12} While isolated single Al atoms and Al pairs of Al–OH–Si–O–Si–OH–Al sequences located in one 6-ring or 8-ring are generally present in the framework of pentasil-ring zeolites,^{28,43,45–48} close unpaired Al atoms (close Al atoms compensated by a [Co(II)(H₂O)₆]²⁺ complex in hydrated zeolites but unable to balance a bare divalent cation in dehydrated zeolites) were reported at higher concentrations exclusively for beta zeolites^{12,48–52} and, moreover, the SSZ-13 zeolite (54% of Al),³¹ which, however, does not belong to the pentasil-ring zeolites. We therefore propose that close unpaired Al atoms, which predominate in the beta zeolite studied (68% of Al),¹² are responsible for the formation of the Al_{FR} Lewis sites in the beta zeolite. Close unpaired Al atoms were unambiguously attributed to Al–OH–Si–O–Si–O–Si–OH–Al sequences in the SSZ-13 zeolite.³¹ Therefore, we assume that the close unpaired Al atoms most likely correspond to Al–OH–Si–O–Si–O–Si–OH–Al sequences located in 12-rings of the *BEA framework. It should be noted that since there are two polymorphs of the *BEA structure, each having nine crystallographically distinguishable T sites, more different AlSi₃Al sequences (i.e., the Al atoms occupy different crystallographically distinguishable T sites) can participate in the formation of the Al_{FR} Lewis sites. This can result in the creation of several Al_{FR} Lewis sites with slightly different local structures exhibiting various locations in the zeolite channel system, resulting in slight variations of their spectroscopic parameters. However, since the Al siting in the investigated beta zeolite is unknown, we cannot determine which AlSi₃Al sequences participate in the formation of the Al_{FR} Lewis sites. This absence of knowledge, nevertheless, has no effect on our analyses of the experimental measurements. Moreover, a possibility that the close unpaired Al atoms relate to

Al–OH–(Si–O)₃–Si–OH–Al sequences located in 12-rings is also considered.

Based on the experimental results revealing neither dealumination nor desilication and, furthermore, our DFT calculations and assumption regarding the presence of Al–OH–Si–O–Si–O–Si–OH–Al sequences (i.e., close unpaired Al atoms) in beta zeolites, we propose the formation of Al_{FR} Lewis sites from two Brønsted acid sites separated by three Si atoms (i.e., Al'–OH–Si'–O–Si''–O–Si'''–OH–Al'') including four steps (see mechanism I in Scheme I) as follows:

- (Step 1) Dehydroxylation of one Brønsted acid site of an Al'–OH–Si'–O–Si''–O–Si'''–OH–Al'' sequence located in a 12-ring to yield Al'_{TRI} Si'⁺–O–Si''–O–Si'''–OH–Al''. An electron-pair acceptor tricoordinated Al'_{TRI} atom is formed.
- (Step 2) Deprotonation of the other Brønsted acid site of Al'_{TRI} Si'⁺–O–Si''–O–Si'''–OH–Al'' to give Al'_{TRI} Si'⁺–O–Si''–O–Si'''–O–Al''⁻.
- (Step 3) Cleavage of two Si'–O bonds and a partial release of the Si' atom from the zeolite framework. The two unsaturated silicon atoms yield two SiOH groups by interactions with residual water molecules. These reaction steps result in a creation of a hole with a nest of two silanol groups in the vicinity of the tricoordinated Al'_{TRI} atom, making it accessible for probes and reactants.
- (Step 4) Subsequent formation of a 3-ring. The positively charged Si' atom forms a bond with the O atom of the deprotonated negatively charged Si''–O–Al''⁻ Brønsted site, and the Al''–O bond is cleaved. However, due to the spatial proximity of the O and Al''_{TRI} atoms, the O atom interacts with one of its lone pairs with the tricoordinated Al''_{TRI} atom and saturates it. This Al''_{TRI} atom tricoordinated to the zeolite framework does not act as an electron-pair acceptor. The Si'' and Si''' atoms preserve their positions in the framework. The unsaturated Si' atom yields a Si(OH)₂ group by reactions with residual water molecules.

In addition, we also considered mechanism II (Scheme II): a cleavage of two Si'–O bonds and two Si''–O bonds and a partial

release of the Si' and Si'' atoms from the zeolite framework in step 3.

Consequently, a 3-ring is formed in step 4, and only the Si''' atom preserves its position in the framework. The Al''_{TRI} atom tricoordinated to the zeolite framework is not accessible due to the coordination of a lone pair of an oxygen atom of the 3-ring. However, the number of silanol groups formed by reactions of unsaturated silicon atoms is doubled [four SiOH and two Si(OH)₂].

Similarly, mechanism III (Scheme SIII of the [supplementary material](#)) involving Al–OH–(Si–O)₃–Si–OH–Al sequences located in 12-rings is considered as well.

We employed ²⁷Al WURST-QCPMG, ¹H MAS, and ²⁹Si MAS NMR spectroscopy to support the suggested mechanisms and determine the number of partially released Si atoms and thus resolve which one of the two mechanisms better describes the formation of Al_{FR} Lewis sites in beta zeolites. The standard way of the detection of Al_{FR} Lewis sites represents FTIR spectroscopy. However, the formation of Al_{FR} Lewis sites cannot be identified directly, but adsorbed acetonitrile-*d*₃ is used as a probe. To allow for comparison between ²⁷Al WURST-QCPMG NMR experiments and the FTIR measurements, acetonitrile-*d*₃ was adsorbed on the dehydrated H-BEA sample. The formation of Al_{FR} Lewis sites in the dehydrated H-BEA sample is reflected in extremely broad ²⁷Al NMR resonances in the ²⁷Al WURST-QCPMG NMR spectrum (Fig. 2).

The ²⁷Al WURST-QCPMG NMR spectrum was simulated using the DFT calculated NMR parameters for the Al'_{TRI} atom with adsorbed CD₃CN and Al''_{TRI} atoms (Table II). Furthermore, there are also Brønsted acid SiOHAl groups present in the framework of the studied zeolite (Table I). It is sufficient to use one ²⁷Al NMR resonance corresponding to the Brønsted acid sites in our simulation. However, our simulation required another ²⁷Al NMR resonance (i.e., the R-IV resonance) to obtain good agreement between the simulated and measured spectra. The DFT calculated NMR parameters were used as the starting values to perform the simulation during which the NMR parameters were slightly optimized to obtain the best fit. The observed NMR parameters are shown in Table II. The experimental NMR parameters of the R-I (assigned to Al'_{TRI}

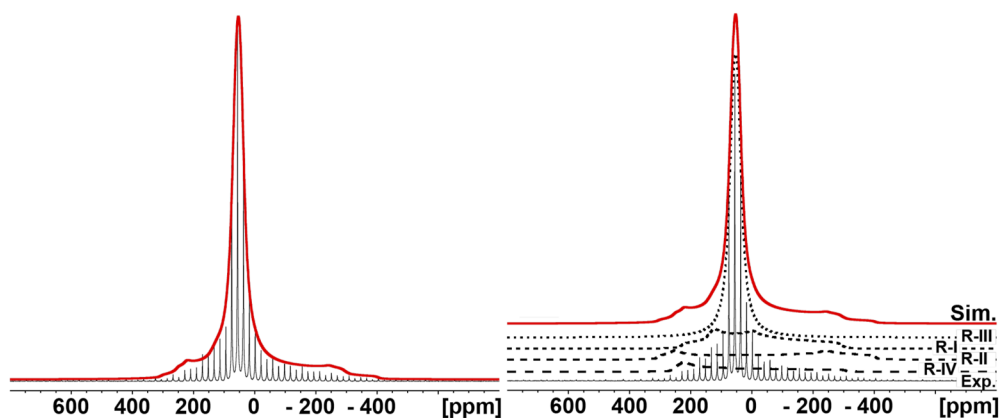


FIG. 2. ²⁷Al WURST-QCPMG NMR spectrum of the dehydrated H-BEA zeolite with adsorbed acetonitrile-*d*₃ (left) and its simulation with the individual ²⁷Al NMR resonances (right).

TABLE II. The calculated and observed values of the ^{27}Al isotropic chemical shift (δ_{iso}), the nuclear quadrupolar coupling constant (C_Q), the asymmetry parameter (η), the span (Ω), the skew (κ), the Euler angles (α , β , and γ), and the intensity. Italicface denotes DFT calculated values.

Atom		δ_{iso} (ppm)	C_Q (MHz)	η	Ω (ppm)	κ	α (deg)	β (deg)	γ (deg)	Intensity (%)
$\text{Al}' + \text{CD}_3\text{CN}$	<i>DFT</i>	65	15.3	0.53	87	-0.3	72	83	353	
	R-I	70 ± 5	14 ± 2	0.7 ± 0.2	74	-0.2	80	0	0	19
Al'	<i>DFT</i>	90	37.2	0.14	126	-0.4	80	89	359	
	Not observed									
$\text{Al}' + \text{N}_2$	<i>DFT</i>	68	28.2	0.25	126	-0.5	74	87	357	
	Not observed									
$\text{Al}' + \text{H}_2\text{O}$	<i>DFT</i>	69	12.6	0.65	70	-0.2	81	85	357	
	R-I	70 ± 5	13 ± 2	0.9 ± 0.2	74	-0.2	80	0	0	22
Al'' (CD_3CN model)	<i>DFT</i>	70	17.3	0.1	69	-0.6	269	89	3	
	R-II	70 ± 5	19 ± 2	0.2 ± 0.2	67	-0.6	275	0	200	15
Al'' (H_2O model)	<i>DFT</i>	69	17.6	0.1	68	-0.7	276	88	178	
	R-II	70 ± 5	19 ± 2	0.2 ± 0.2	67	-0.6	275	0	200	18
SiOHAl	<i>DFT</i> ^a	66	3.5	0.85						
	R-III	60 ± 5	3.5 ± 0.5	0.4 ± 0.2						$62,^b 56^c$
Penta-coordinated Al	Not calculated									
	R-IV	40 ± 5	3.5 ± 0.5	0.5 ± 0.2	550	0.87	0	0	0	$4,^b 4^c$

^aBare framework AlO_4^- model without a proton.^b CD_3CN model.^c H_2O model.

with adsorbed acetonitrile- d_3) and R-II (attributed to Al'_{TRI}) resonances are in very good agreement with the DFT calculated values (Table II). It should be noted that several various AlSi_3Al sequences can participate in the formation of the Al_{FR} Lewis sites, and therefore, using additional broad ^{27}Al NMR resonances with close NMR parameters corresponding to the Al'_{TRI} atom with adsorbed CD_3CN and the Al''_{TRI} atom located in various crystallographically distinguishable T sites would be necessary to obtain a perfect fit. However, employing four ^{27}Al NMR resonances for the fit of the ^{27}Al WURST-QCPMG NMR spectrum (Fig. 2) were sufficient for our analysis of the experimental measurements and the support of the suggested mechanism.

While framework Al atoms in hydrated zeolites exhibit very narrow spectra with the C_Q value close to 3 MHz,^{53–55} Al atoms in dehydrated H-zeolites are reflected in significantly wider resonances with the C_Q values ranging from 5 to 16 MHz.^{55–58} This wide range of the C_Q parameters can be explained by the various degrees of the mobility of the Brønsted proton on the AlO_4^- tetrahedra.⁵⁹ Our DFT calculations of the beta zeolite yielded (i) the C_Q ³⁸ value of 4 MHz (Table II) for the bare framework AlO_4^- model without a proton representing the completely mobile Brønsted proton⁵⁵ on AlO_4^- and (ii) the C_Q constant of 17–21 MHz (Table SI of the supplementary material) for the SiOHAl Brønsted acid sites with completely immobile protons. Therefore, the R-III resonance with the measured $C_Q = 3.5$ MHz can be assigned to the Al atoms of Brønsted acid SiOHAl groups with highly mobile protons.

The very low intensity R-IV resonance with an enormous anisotropy of the chemical shift most likely corresponds to a small fraction of penta-coordinated extra-framework Al species forming extra-framework Al_{EF} Lewis sites that are not distinguishable by FTIR from framework Al_{FR} Lewis sites.

Furthermore, the dehydrated H-BEA sample was used to investigate the structure of “bare” Al_{FR} Lewis sites (i.e., without adsorbed acetonitrile- d_3). Again, the “bare” Al_{FR} Lewis sites are reflected in extremely broad ^{27}Al NMR resonances in the ^{27}Al WURST-QCPMG NMR spectrum (Fig. 3).

Our DFT calculations of the C_Q parameters of the Al'_{TRI} and Al''_{TRI} atoms taking part in the formation of Al_{FR} Lewis sites gave the values of 37 (Table II) and 17 MHz, respectively. There is no observed ^{27}Al NMR resonance in the ^{27}Al WURST-QCPMG NMR spectrum (Fig. 3), which can be assigned to Al'_{TRI} with the C_Q value of 37 MHz although the ^{27}Al WURST-QCPMG NMR method guarantees detection of the signal with C_Q up to 50 MHz (details are given in the supplementary material).^{16,60} The discrepancy of the C_Q parameters of the electron-pair acceptor tricoordinated Al'_{TRI} atom can hardly be explained only by the difference between the calculated model and the real structure in the zeolite (it should be noted that there are two polymorphs of the *BEA structure, each having nine crystallographically distinguishable T sites, and therefore, there is a large number of possible AlSi_3Al structures). However, the Al_{TRI} atom tricoordinated to the zeolite framework is extremely reactive and interacts not only with water molecules but even with N_2 present in the zeolite.⁶¹ It should be noted that new SiOH and Si(OH)₂ groups cannot be formed in the absence of water molecules. Our DFT calculations of the C_Q parameters of the Al'_{TRI} of Al_{FR} Lewis sites with adsorbed N_2 and H_2O (Table II) yielded the values of 28 and 13 MHz, respectively (Table II). There is no observed ^{27}Al NMR resonance in the ^{27}Al WURST-QCPMG NMR spectrum of the dehydrated H-BEA zeolite (Fig. 3), which can be assigned to Al'_{TRI} with the C_Q value of 28 MHz. Conversely, the simulation of this spectrum with one ^{27}Al NMR resonance with the C_Q parameters (Table II) 13 MHz (Al'_{TRI} with adsorbed H_2O), one

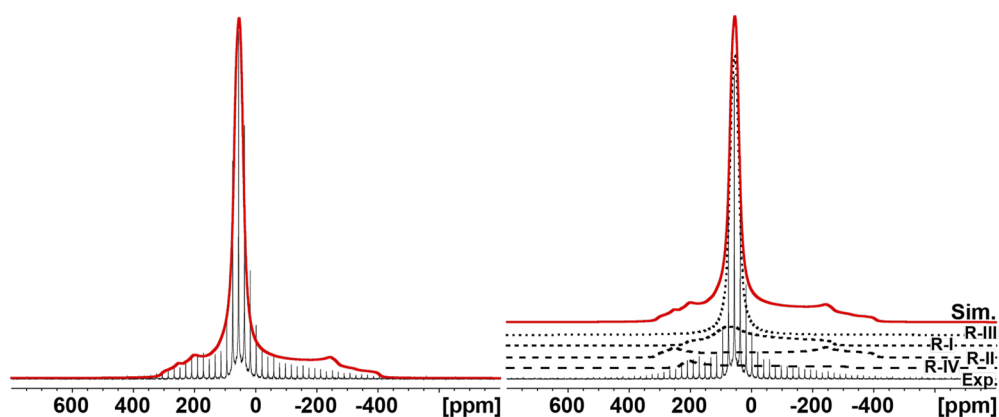


FIG. 3. ^{27}Al WURST-QCPMG NMR spectrum of the dehydrated H-BEA zeolite (left) and its simulation with the individual ^{27}Al NMR resonances (right).

^{27}Al NMR resonance with the C_Q value of 18 MHz (Al''_{TRI}), one ^{27}Al NMR resonance corresponding to the Brønsted acid sites, and another ^{27}Al NMR resonance (i.e., the R-IV resonance) yielded good agreement between the simulated and measured spectra. The DFT calculated NMR parameters were used as the starting values to perform the simulation during which the NMR parameters were slightly optimized to obtain the best fit.

The assignment of the R-I and R-II resonances to the Al'_{TRI} and Al''_{TRI} atoms, respectively, is in good agreement with the results of the quantitative analysis. Our simulation of the ^{27}Al WURST-QCPMG NMR spectrum (Fig. 3) yielded 22% of all the Al atoms for Al'_{TRI} . This value agrees well with the 28% of Al'_{TRI} derived from our FTIR measurements (Table I). It should be noted that FTIR experiments reflect only the accessible Al atoms of the acid sites (i.e., Al'_{TRI}), and therefore, 54 $\mu\text{mol/g}$ of the Brønsted acid SiOHAl groups and 33 $\mu\text{mol/g}$ of Al_{FR} Lewis sites correspond to 54 $\mu\text{mol/g}$ of Al atoms creating the Brønsted acid sites and 33 $\mu\text{mol/g}$ of Al'_{TRI} and 33 $\mu\text{mol/g}$ of Al''_{TRI} (i.e., 66 $\mu\text{mol/g}$ of Al atoms taking part in the formation of the Al_{FR} Lewis sites). Therefore, we can conclude that a water molecule is adsorbed on Al'_{TRI} of the Al_{FR} Lewis site at ambient laboratory temperature (when the ^{27}Al WURST-QCPMG

NMR spectrum was measured). Conversely, probes and reactants can replace H_2O at elevated temperatures under reaction conditions, and therefore, Al'_{TRI} atoms can serve as reaction centers.

The assignments of the R-I and R-II resonances to the Al'_{TRI} and Al''_{TRI} atoms, respectively, were further confirmed by the results of the ^{27}Al BRAIN-CP/WURST-QCPMG NMR experiment, which showed a significant suppression of the R-III resonance in the spectrum (Fig. 4) assigned to the Al atoms of the Brønsted acid SiOHAl groups. Only protons of the Brønsted acid sites should be highly mobile, and the corresponding Al atoms are thus suppressed in the ^{27}Al BRAIN-CP/WURST-QCPMG NMR spectrum even when a relatively short mixing time of 1 ms was employed.

This result most likely indicates the presence of close fixed hydrogens of the water molecule adsorbed on Al'_{TRI} (two fixed hydrogens at 2.5 Å). There is a lower efficiency of the magnetization transfer from hydrogens of silanol groups to Al''_{TRI} due to larger distances of the silanol groups. The R-III resonance with $C_Q = 3.5$ MHz is almost completely suppressed in the ^{27}Al BRAIN-CP/WURST-QCPMG NMR spectrum due to a very low efficiency of magnetization transfer from the SiOHAl groups.

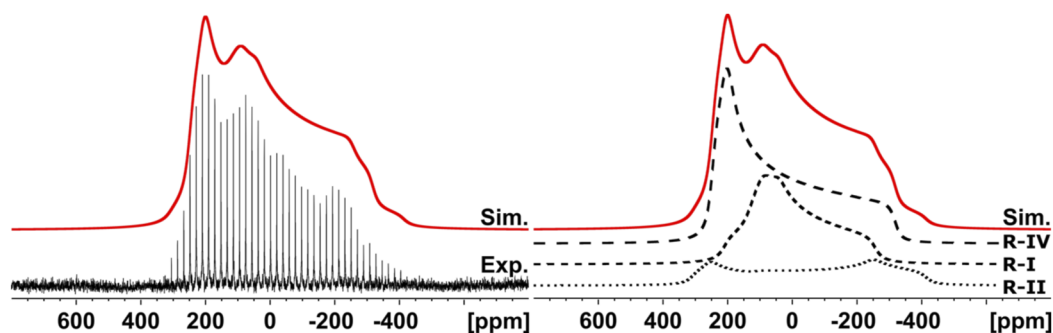


FIG. 4. ^{27}Al BRAIN-CP/WURST-QCPMG NMR spectrum of the dehydrated H-BEA zeolite measured at a relatively short contact time (1 ms) (left) and its simulation with the individual ^{27}Al NMR resonances (right).

It should be noted that ^{27}Al NMR resonances with high C_Q values can also relate to Al atoms of Brønsted acid SiOHAl groups with completely immobile protons.⁶² Nevertheless, neither the R-I resonance nor the R-II resonance can correspond to Al atoms of the Brønsted acid SiOHAl groups since our FTIR experiments show that 28% of the acid sites correspond to Al_{FR} Lewis sites and the rest are Brønsted acid sites (Table I), and there is no other observed ^{27}Al NMR resonance in the ^{27}Al WURST-QCPMG NMR spectrum with a larger C_Q value.

^1H MAS and ^{29}Si MAS NMR experiments were employed to determine the number of partially released Si atoms (Scheme I and II). Mechanisms I and II differ in the number of Si atoms with OH groups and number of OH groups. It is very difficult to distinguish between Si(3Si,1OH) and Si(2Si,2OH) atoms in ^{29}Si MAS NMR spectra of the beta zeolite composed of two polymorphs each possessing 9 crystallographically distinguishable T sites. Conversely, ^1H MAS NMR spectroscopy does not suffer from this issue and therefore represents a promising tool to identify the number of partially released Si atoms.

The ^1H MAS NMR spectrum of the dehydrated H-BEA zeolite (Fig. 1) shows three ^1H NMR resonances: (i) a dominant one centered around 1.6 ppm, corresponding to the silanol SiOH groups, (ii) another resonance at around 3.8 ppm, relating to the Brønsted acid SiOHAl groups with a shoulder at around 5 ppm, which can likely be attributed to adsorbed water molecules, and (iii) a minor resonance at 6.3, which most likely can be assigned to residual NH_4^+ cations.⁶³ These results agree well with the FTIR spectrum of the dehydrated H-BEA samples in the region of OH vibrations (Fig. S2 of the supplementary material). The FTIR spectrum clearly shows the bands corresponding to the OH vibrations of SiOH and SiOHAl; however, it does not allow for quantification of the OH groups. Nevertheless, the concentration of the OH groups can be estimated from the ^1H MAS NMR spectrum calibrated using FTIR spectroscopy of adsorbed acetonitrile- d_3 on the Brønsted SiOHAl sites. The concentrations of the OH groups are listed in Table I.

Figure 5 compares the ^{29}Si MAS NMR spectra of the hydrated NH_4 -BEA sample and the H-BEA zeolite dehydrated at 500 °C and their simulations (with the lowest possible number of resonances) and reveals (i) a significant increase in either one of the Si(3Si,1OH) and Si(2Si,2OH) atoms or both of them from 6% to 11% of all the Si atoms (Fig. 5 and Table I) with a new silanol resonance at -106.5 ppm, which is a product of a partial release of Si atoms (Schemes I and II) analogous to a formation of silanol nests,^{64,65} and (ii) an appearance of a new ^{29}Si NMR resonance at -120.5 ppm. The assignment of ^{29}Si NMR resonances to silanols was based on the ^{29}Si CP MAS NMR experiment (Fig. S7 of the supplementary material).

Since the ^{29}Si NMR resonance at -120.5 ppm is within the range of ^{29}Si chemical shifts of Si(4Si), it most likely corresponds to framework Si(4Si) atoms that rearranged when the framework was perturbed.

Quantifications of (i) the Si atoms of the SiOH and Si(OH)₂ groups created during the formation of the Al_{FR} Lewis sites by ^{29}Si MAS NMR spectroscopy and (ii) the corresponding H atoms of these SiOH and Si(OH)₂ groups employing ^1H MAS NMR spectroscopy were used to determine the number of Si atoms partly released from the framework.

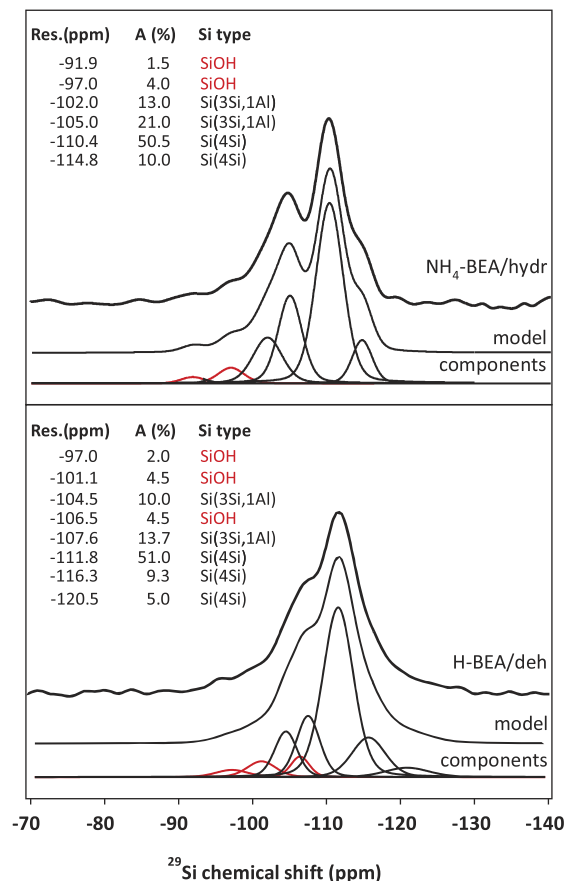


FIG. 5. ^{29}Si MAS NMR spectra of the hydrated NH_4 -BEA (top) and dehydrated H-BEA (bottom) zeolites and their simulations.

Comparison between (i) the concentrations of the $\text{Si}(\text{OH})_{1,2}$ atoms and the OH groups measured for the H-BEA sample dehydrated at 500 °C and (ii) the corresponding theoretical values derived from the suggested mechanisms for one and two Si atoms partly released from the framework (Schemes I and II, respectively) indicates that the former mechanism (i.e., a partial release of only one silicon atom) is in significantly better agreement with the experimental results than the latter (Table I).

The possibility of existence of the zeolite framework with stable either the 3-ring or the 4-ring and tricoordinated Al_{FR} atoms as well as the accessibility of these Al atoms were investigated by extensive DFT calculations including molecular dynamics. The computational results reveal that the formed 3-ring (Schemes I and II) and 4-ring (Scheme SIII of the supplementary material) can be created and are stable and one Al_{TRI} is accessible for a CD_3CN probe while the other Al_{TRI} is closed for donor molecules due to its donor-acceptor interaction with an electron-pair of one of the oxygen atoms of the 3-ring or 4-ring. Since mainly only one silicon atom is partly released (Table I), a possibility that Al_{FR} Lewis sites are predominantly formed from $\text{Al}-\text{OH}-(\text{Si}-\text{O})_3-\text{Si}-\text{OH}-\text{Al}$ sequences located in 12-rings (mechanism III in Scheme SIII of

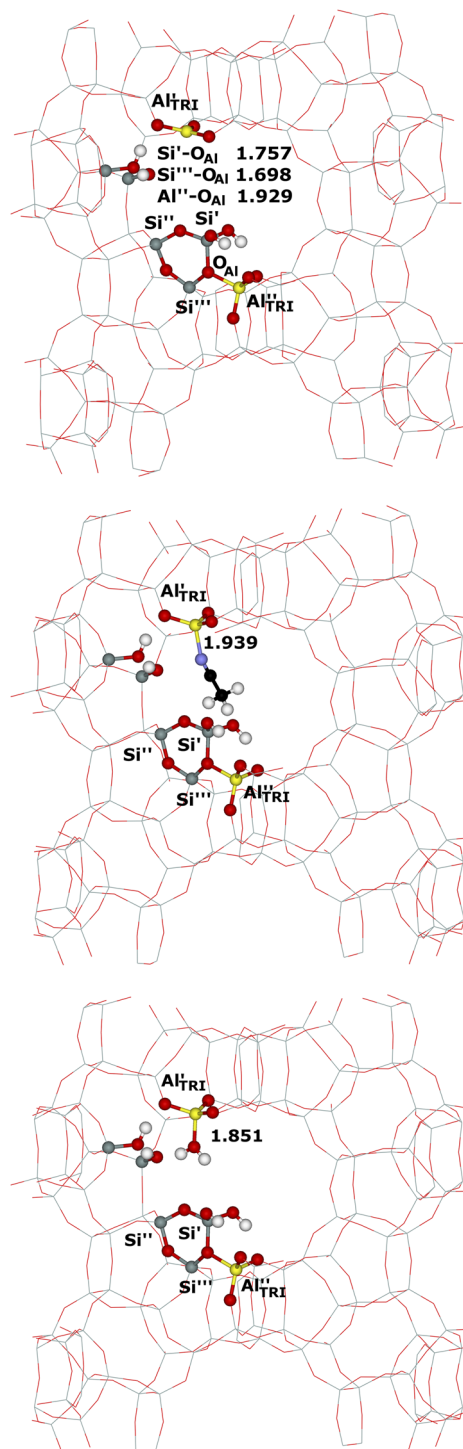


FIG. 6. The optimized structures of the model of the Al_{FR} Lewis site with one Si atom partly released from the zeolite framework (mechanism I) (top) and acetone (middle) and water (bottom) adsorbed on the Al'_{TRI} atom of the same model of the Al_{FR} Lewis site. The atoms of interest are displayed as balls. The distances are in Å. Silicon atoms are in gray, oxygen atoms in red, aluminum atoms in yellow, nitrogen atoms in blue, and hydrogen atoms in white.

the [supplementary material](#)) can be ruled out. Our DFT calculations show that a 4-ring cannot be formed if only one Si atom is partly released from the framework. Mechanism III requires a partial release of the Si' and Si'' atoms from the zeolite framework and yields a $(\text{Si}-\text{O})_4$ 4-ring with the Si''' and Si'''' atoms preserving their positions in the framework and eight silanol groups. Therefore, $\text{Al}-\text{OH}-(\text{Si}-\text{O})_3-\text{Si}-\text{OH}-\text{Al}$ sequences can be excluded as the main precursors of the Al_{FR} Lewis sites. It should be noted that $\text{Al}-\text{OH}-\text{Si}-\text{O}-\text{Si}-\text{OH}-\text{Al}$ sequences cannot represent precursors of the Al_{FR} Lewis sites either because 2-rings cannot exist in the framework. Therefore, we propose that Al_{FR} Lewis sites are predominantly formed from $\text{Al}-\text{OH}-(\text{Si}-\text{O})_2-\text{Si}-\text{OH}-\text{Al}$ sequences (corresponding to the close unpaired Al atoms) from which one Si atom is partly released (Scheme I). The calculated arrangement of the Al_{FR} Lewis site is depicted in Fig. 6.

V. DISCUSSION

The proposed reaction steps are consistent with all our experimental measurements on the H-BEA sample. At least one Si atom must be partly released from the framework to allow for the formation of a hole in the vicinity of the tricoordinated Al'_{TRI} atom; otherwise, Al'_{TRI} would not be accessible for probes and reactants. If the Si' atom did not form a ring with the Si''' atom, then it would either be fully released from the framework to yield $\text{Si}(\text{OH})_4$ or form a $-\text{Si}(\text{OH})_3$ group attached to the framework by one Si-O bond. Our ^{29}Si MAS NMR experiments show the presence of neither $\text{Si}(1\text{Si},3\text{OH})$ nor $\text{Si}(0\text{Si},4\text{OH})$ atoms in the calcined sample. Furthermore, if some Si species were completely released from the framework, then it would be difficult to explain the reversibility of the formation of the Al_{FR} Lewis sites, i.e., that tetrahedral Al atoms are created from Al_{FR} Lewis sites upon rehydration of the samples and also the preservation of the Si/Al ratio of (i) the hydrated parent sample (NH_4 -BEA), (ii) the calcined and rehydrated sample (H-BEA), and (iii) the calcined, rehydrated, and subsequently equilibrated with NaNO_3 sample (NaH-BEA) (Fig. S5 of the [supplementary material](#)).¹² In addition, the formation of the ring prevents the reprotonation of the deprotonated $\text{Si}'''-\text{O}-\text{Al}''$ Brønsted site, and thus, one Al_{FR} Lewis site is formed at the expense of two Brønsted acid sites as observed.

The fact that $\text{Al}-\text{OH}-(\text{Si}-\text{O})_2-\text{Si}-\text{OH}-\text{Al}$ sequences located in 12-rings most likely represent the precursors of the Al_{FR} Lewis sites explains why the *BEA structure is very unique regarding the massive formation of Al_{FR} Lewis sites at lower temperatures. These close unpaired Al atoms were reported at higher concentrations only for the beta^{9,12} and SSZ-13³¹ zeolites. Nevertheless, the above suggestion indicates that Al_{FR} Lewis sites are formed in other zeolites than the beta and SSZ-13 zeolites by different mechanisms as it was confirmed for ferrierite.⁸

VI. CONCLUSIONS

Our study suggests that $\text{Al}-\text{OH}-\text{Si}-\text{O}-\text{Si}-\text{O}-\text{Si}-\text{OH}-\text{Al}$ sequences located in 12-rings most likely represent the main precursors of the Al_{FR} Lewis sites in beta zeolites. Two Si-O and two Al-O bonds are cleaved to yield (i) a partly released Si atom from the zeolite framework, which subsequently creates a 3-ring, (ii) four silanol groups, and (iii) two electron-pair acceptor Al'_{TRI}

atoms. The production of the 3-ring creates a hole with a nest of two silanol groups in the vicinity of one Al'_{TRI} atom, making it accessible for electron-pair donors while the other Al''_{TRI} atom is closed. Therefore, the two Al_{TRI} atoms correspond to one Al_{FR} Lewis site. Our results show that the electron-pair acceptor of Al_{FR} Lewis sites corresponds to an Al'_{TRI} atom tricoordinated to the zeolite framework, which adsorbs a water molecule. The Al'_{TRI} atoms with adsorbed H_2O and Al''_{TRI} are reflected in two extremely broad ^{27}Al NMR resonances—one with $\delta_i = 70 \pm 5$ ppm, $C_Q = 13 \pm 2$ MHz, and $\eta = 0.9 \pm 0.2$ and the other one with $\delta_i = 70 \pm 5$ ppm, $C_Q = 19 \pm 2$ MHz, and $\eta = 0.2 \pm 0.2$, respectively. Adsorption of acetonitrile- d_3 on the zeolite permitted comparison between the ^{27}Al WURST-QCPMG NMR measurements and the FTIR experiments used to evidence and quantify the Al_{FR} Lewis sites. The observed ^{27}Al NMR resonances are again extremely broad—one corresponding to Al'_{TRI} with adsorbed acetonitrile- d_3 with $\delta_i = 70 \pm 5$ ppm, $C_Q = 14 \pm 2$ MHz, and $\eta = 0.7 \pm 0.2$ and the other one related to Al''_{TRI} with $\delta_i = 70 \pm 5$ ppm, $C_Q = 19 \pm 2$ MHz, and $\eta = 0.2 \pm 0.2$. The partial release of one Si atom from the zeolite framework is proposed as a key step for the formation of stable and especially accessible Al_{FR} Lewis sites.

SUPPLEMENTARY MATERIAL

See the [supplementary material](#) for additional figures, a table, and experimental sections.

ACKNOWLEDGMENTS

This work was supported by the Grant Agency of the Czech Republic (Grant No. GA 19-05259S) and Grant NOs. RVO:61388955 and RVO:61389013. This work was supported by the Ministry of Education, Youth and Sports of the Czech Republic through the e-INFRA CZ (No. 90140). We thank Professor Robert W. Schurko of the University of Windsor, Canada, for providing us the BRAIN-CP/WURST-CPMG pulse sequence.

AUTHOR DECLARATIONS

Conflict of Interest

The authors have no conflicts to disclose.

DATA AVAILABILITY

The data that support the findings of this study are available from the corresponding author upon reasonable request.

REFERENCES

- I. Kiricsi, C. Flego, G. Pazzuconi, W. O. Parker, Jr., R. Millini, C. Perego, and G. Bellussi, *J. Phys. Chem.* **98**, 4627–4634 (1994).
- J. Čejka and B. Wichterlová, *Catal. Rev.: Sci. Eng.* **44**, 375–421 (2002).
- A. Corma and H. García, *Chem. Rev.* **102**, 3837–3892 (2002).
- A. Corma, *Chem. Rev.* **95**, 559–614 (1995).
- O. Bortnovsky, Z. Sobalik, and B. Wichterlová, *Microporous Mesoporous Mater.* **46**, 265–275 (2001).
- F. Collignon, P. A. Jacobs, P. Grobet, and G. Poncelet, *J. Phys. Chem. B* **105**, 6812–6816 (2001).
- J. A. van Bokhoven, A. M. J. van der Eerden, and D. C. Koningsberger, *J. Am. Chem. Soc.* **125**, 7435–7442 (2003).
- J. Brus, L. Kobera, W. Schoefberger, M. Urbanová, P. Klein, P. Sazama, E. Tabor, S. Sklenak, A. V. Fishchuk, and J. Dědeček, *Angew. Chem., Int. Ed.* **54**, 541–545 (2015).
- O. Bortnovsky, Z. Sobalik, B. Wichterlová, and Z. Bastl, *J. Catal.* **210**, 171–182 (2002).
- A. Zecchina, S. Bordiga, G. Spoto, D. Scarano, G. Petrini, G. Leofanti, M. Padovan, and C. O. Areà, *J. Chem. Soc., Faraday Trans.* **88**, 2959–2969 (1992).
- P. J. Kunkeler, B. J. Zuurdeeg, J. C. van der Waal, J. A. van Bokhoven, D. C. Koningsberger, and H. van Bekkum, *J. Catal.* **180**, 234–244 (1998).
- P. Sazama, E. Tabor, P. Klein, B. Wichterlová, S. Sklenak, L. Mokrzycki, V. Pashkova, M. Ogura, and J. Dedecek, *J. Catal.* **333**, 102–114 (2016).
- J. C. van der Waal, E. J. Creighton, P. J. Kunkeler, K. Tan, and H. van Bekkum, *Top. Catal.* **4**, 261–268 (1997).
- B. Wichterlová, Z. Tvarůžková, Z. Sobalik, and P. Sarv, *Microporous Mesoporous Mater.* **24**, 223–233 (1998).
- D. Massiot, F. Fayon, M. Capron, I. King, S. Le Calvé, B. Alonso, J.-O. Durand, B. Bujoli, Z. Gan, and G. Hoatson, *Magn. Reson. Chem.* **40**, 70–76 (2002).
- L. A. O'Dell, A. J. Rossini, and R. W. Schurko, *Chem. Phys. Lett.* **468**, 330–335 (2009).
- K. J. Harris, A. Lupulescu, B. E. G. Lucier, L. Frydman, and R. W. Schurko, *J. Magn. Reson.* **224**, 38–47 (2012).
- G. Kresse and J. Hafner, *Phys. Rev. B* **48**, 13115–13118 (1993).
- G. Kresse and J. Hafner, *Phys. Rev. B* **49**, 14251–14269 (1994).
- G. Kresse and J. Furthmüller, *Phys. Rev. B* **54**, 11169–11186 (1996).
- G. Kresse and J. Furthmüller, *Comput. Mater. Sci.* **6**, 15–50 (1996).
- P. E. Blöchl, *Phys. Rev. B* **50**, 17953–17979 (1994).
- G. Kresse and D. Joubert, *Phys. Rev. B* **59**, 1758–1775 (1999).
- J. P. Perdew, J. A. Chevary, S. H. Vosko, K. A. Jackson, M. R. Pederson, D. J. Singh, and C. Fiolhais, *Phys. Rev. B* **46**, 6671–6687 (1992).
- J. P. Perdew and Y. Wang, *Phys. Rev. B* **45**, 13244–13249 (1992).
- L. Benco, T. Bucko, R. Grybos, J. Hafner, Z. Sobalik, J. Dedecek, S. Sklenak, and J. Hrusak, *J. Phys. Chem. C* **111**, 9393–9402 (2007).
- S. Sklenak, P. C. Andrikopoulos, B. Boekfa, B. Jansang, J. Nováková, L. Benco, T. Bucko, J. Hafner, J. Dědeček, and Z. Sobalik, *J. Catal.* **272**, 262–274 (2010).
- S. Sklenak, P. C. Andrikopoulos, S. R. Whittleton, H. Jirglova, P. Sazama, L. Benco, T. Bucko, J. Hafner, and Z. Sobalik, *J. Phys. Chem. C* **117**, 3958–3968 (2013).
- P. C. Andrikopoulos, Z. Sobalik, J. Novakova, P. Sazama, and S. Sklenak, *ChemPhysChem* **14**, 520–531 (2013).
- R. Karcz, J. Dedecek, B. Supronowicz, H. M. Thomas, P. Klein, E. Tabor, P. Sazama, V. Pashkova, and S. Sklenak, *Chem. - Eur. J.* **23**, 8857–8870 (2017).
- K. Mlekodaj, J. Dedecek, V. Pashkova, E. Tabor, P. Klein, M. Urbanova, R. Karcz, P. Sazama, S. R. Whittleton, H. M. Thomas, A. V. Fishchuk, and S. Sklenak, *J. Phys. Chem. C* **123**, 7968–7987 (2019).
- S. Nosé, *J. Chem. Phys.* **81**, 511–519 (1984).
- L. Verlet, *Phys. Rev.* **159**, 98–103 (1967).
- L. Verlet, *Phys. Rev.* **165**, 201–214 (1968).
- P. Klein, J. Dedecek, H. M. Thomas, S. R. Whittleton, V. Pashkova, J. Brus, L. Kobera, and S. Sklenak, *Chem. Commun.* **51**, 8962–8965 (2015).
- E. Tabor, M. Lemishka, Z. Sobalik, K. Mlekodaj, P. C. Andrikopoulos, J. Dedecek, and S. Sklenak, *Commun. Chem.* **2**, 71 (2019).
- M. J. Frisch *et al.*, Gaussian 09, Revision C.01, Gaussian, Inc., Wallingford, CT, 2011.
- S. Adiga, D. Aebi, and D. L. Bryce, *Can. J. Chem.* **85**, 496–505 (2007).
- K. Wolinski, J. F. Hinton, and P. Pulay, *J. Am. Chem. Soc.* **112**, 8251–8260 (1990).
- C. Lee, W. Yang, and R. G. Parr, *Phys. Rev. B* **37**, 785–789 (1988).
- A. D. Becke, *J. Chem. Phys.* **98**, 5648–5652 (1993).
- F. Jensen, *J. Chem. Theory Comput.* **4**, 719–727 (2008).
- S. Sklenak, J. Dědeček, C. Li, B. Wichterlová, V. Gábová, M. Sierka, and J. Sauer, *Phys. Chem. Chem. Phys.* **11**, 1237–1247 (2009).

- ⁴⁴J. Dědeček, S. Sklenak, C. Li, F. Gao, J. Brus, Q. Zhu, and T. Tatsumi, *J. Phys. Chem. C* **113**, 14454–14466 (2009).
- ⁴⁵S. Sklenak, J. Dědeček, C. Li, B. Wichterlová, V. Gábová, M. Sierka, and J. Sauer, *Angew. Chem., Int. Ed.* **46**, 7286–7289 (2007).
- ⁴⁶J. Dědeček, S. Sklenak, C. Li, B. Wichterlová, V. Gabová, J. Brus, M. Sierka, and J. Sauer, *J. Phys. Chem. C* **113**, 1447–1458 (2009).
- ⁴⁷J. Dědeček, M. J. Lucero, C. Li, F. Gao, P. Klein, M. Urbanova, Z. Tvaruzkova, P. Sazama, and S. Sklenak, *J. Phys. Chem. C* **115**, 11056–11064 (2011).
- ⁴⁸J. Dědeček, Z. Sobalík, and B. Wichterlová, *Catal. Rev.: Sci. Eng.* **54**, 135–223 (2012).
- ⁴⁹J. Dědeček, L. Čapek, D. Kaucký, Z. Sobalík, and B. Wichterlová, *J. Catal.* **211**, 198–207 (2002).
- ⁵⁰L. Čapek, J. Dědeček, P. Sazama, and B. Wichterlová, *J. Catal.* **272**, 44–54 (2010).
- ⁵¹J. Dědeček, L. Čapek, P. Sazama, Z. Sobalík, and B. Wichterlová, *Appl. Catal., A* **391**, 244–253 (2011).
- ⁵²J. Dědeček, E. Tabor, and S. Sklenak, *ChemSusChem* **12**, 556–576 (2019).
- ⁵³J. A. van Bokhoven, D. C. Koningsberger, P. Kunkeler, H. van Bekkum, and A. P. M. Kentgens, *J. Am. Chem. Soc.* **122**, 12842–12847 (2000).
- ⁵⁴J. Kanellopoulos, A. Unger, W. Schwieger, and D. Freude, *J. Catal.* **237**, 416–425 (2006).
- ⁵⁵P. Klein, V. Pashkova, H. M. Thomas, S. R. Whittleton, J. Brus, L. Kobera, J. Dedecek, and S. Sklenak, *J. Phys. Chem. C* **120**, 14216–14225 (2016).
- ⁵⁶D. Freude, H. Ernst, and I. Wolf, *Solid State Nucl. Magn. Reson.* **3**, 271–286 (1994).
- ⁵⁷J. Jiao, S. Altwasser, W. Wang, J. Weitkamp, and M. Hunger, *J. Phys. Chem. B* **108**, 14305–14310 (2004).
- ⁵⁸J. Jiao, J. Kanellopoulos, W. Wang, S. S. Ray, H. Foerster, D. Freude, and M. Hunger, *Phys. Chem. Chem. Phys.* **7**, 3221–3226 (2005).
- ⁵⁹M. Sierka and J. Sauer, *J. Phys. Chem. B* **105**, 1603–1613 (2001).
- ⁶⁰L. Kobera, J. Czernek, S. Abbrent, H. Mackova, L. Pavlovec, J. Rohlicek, and J. Brus, *Inorg. Chem.* **57**, 7428–7437 (2018).
- ⁶¹R. Wischert, C. Copéret, F. Delbecq, and P. Sautet, *Chem. Commun.* **47**, 4890–4892 (2011).
- ⁶²A. P. M. Kentgens, D. Iuga, M. Kalwei, and H. Koller, *J. Am. Chem. Soc.* **123**, 2925–2926 (2001).
- ⁶³M. Hunger, *Catal. Rev.: Sci. Eng.* **39**, 345–393 (1997).
- ⁶⁴R. Hajjar, Y. Millot, P. P. Man, M. Che, and S. Dzwigaj, *J. Phys. Chem. C* **112**, 20167–20175 (2008).
- ⁶⁵S. M. Maier, A. Jentys, and J. A. Lercher, *J. Phys. Chem. C* **115**, 8005–8013 (2011).